Submitted: 10/01/15
Accepted: 20/02/15

Research Article

[1]Department of Physics, McGill University, Montreal, QC, Canada
[2]Department of Biomedical Engineering, McGill University, Montreal, QC, Canada

Keywords

Digital holography: a numerical reconstruction of a scene captured through interferometry, which presents multiple perspective of the scene in 3-D space

Mach-Zehnder interferometer: a device that extracts spatial information from an object using two split beams, whose phase-shift after reflection reveals the depth from a light source to the object

Email Correspondence

bimochan.niraula@mail.mcgill.ca

Bimochan Niraula[1], Jay L. Nadeau[2]

Optimisation of a Holographic Microscope for Microbial Study

Abstract

Background: Tracking of microbial organisms over a volume requires images at multiple focal planes along the orthogonal direction. With most conventional microscopes, this requires repeated readjustments; using Digital Holographic Microscopy (DHM), it is possible to use a set of interference patterns to reconstruct at various distances, thereby creating a 3D stack based off a single image.

Methods: We used an off-axis Mach-Zehnder DHM for imaging and tracking bacterial movement. We describe the algorithm employed for tracking, as well as our improvement of trackability by testing differences in image contrast with the use of Quantum Dots.

Results: We show that the use of Quantum Dots resulted in an increase in contrast of approximately 11%.

Conclusion: We suggest this as a method of increasing resolvability of individual microbes. With a more compact design, the microscope will be applicable in various fields, and can be used remotely for studies of microbial organisms.

Introduction

Digital Holographic Microscopy (DHM) implementations use coherent interference between a clear "reference" beam and an "object" beam transmitted through, or reflected by, a sample of interest. This encodes the complex wavefront (amplitude and phase) as intensity modulations (fringes) on the detector plane. (1-4) Following this physical recording, the reconstruction process can be undertaken on a computer as a post-processing step. The encoded object wavefront of interest is retrieved from the digital hologram, and can be numerically propagated to any plane of interest using Fresnel Algorithms or Rayleigh-Sommerfield diffraction formula. (5-8) Finally, the amplitude and phase components of the complex wavefront in the target plane are computed to be saved for later analysis. The post-processing propagation procedure can be run repeatedly with different propagation distances to build a 3-D stack from a singly acquired hologram for each timeframe, without the need to scan in depth. .

Instrument & Samples

Microscope Configuration

The microscope used was a dual-beam off-axis Mach-Zehnder (MZ) type of DHM configuration, using a magnifying lens to reach the targeted sub-micron lateral resolution required for bacterial imaging (Fig. 1).

A blue λ= 405 nm laser was used as the coherent light source. The camera used was a 2448 x 2050 CCD with 3.45 µm pixel size, delivering up to 22 fps in 1024 x 1024 (1 Mpx) mode and 14 fps with 2048 x 2048 pixels (4 Mpx). Using a Thorlabs Geltech® aspheric lens (focal length = 8 mm and NA of 0.5) as a magnification M = 20x single-lens objective, we achieved a design field-of-view (FOV) of about 0.35 x 0.35 mm2. For high-speed hologram reconstruction, we employed the LynceeTec Koala® off-axis DHM reconstruction software. (9)

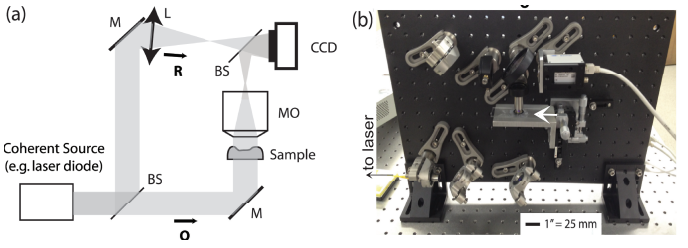

Figure 1. Instrument design. (a) General schematic showing a typical Mach-Zehnder off-axis DHM scheme. Legend: O, Object beam; R, Reference beam; BS, Beamsplitter; M, Mirrors; L, Lens; MO, Microscope Objective. (b) Photo of the actual breadboard instrument, with its fibered laser diode source injected in the bottom left.

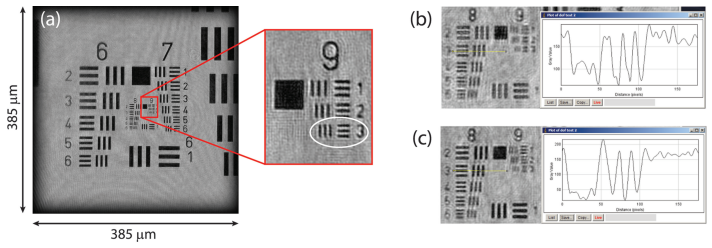

Figure 2. MZ-DHM optical performances assessment with a USAF test target sample. (a) Intensity-reconstruction image, with the inset zooming on the highest resolution elements: the white circle indicates 0.78 μm-wide scale bars; (b,c) Zoomed images on the smallest elements (groups 8 and 9) of (a), but reconstructed for the target moved along the optical axis (focus) by -1 mm (b) or +1 mm (c) away from the nominal working distance used in (a): the 3rd element of group 8 (1.55 μm-wide) is still well resolved in both case as shown in the cross-profiles, indicating less than a loss of less than factor two in resolution vs. the nominal 0.8 μm.

Using a NIST-compliant high-resolution USAF test target as a sample (Fig. 2), we measured a lateral FOV of 0.385 x 0.385 mm2 over 1980 x 1980 pixels indicative of an effective magnification of about 18x (Fig. 2a). The target was also vertically shifted from the nominal focal height and the contrast ratio of the target elements were compared to receive a depth of focus in z (Fig. 2b, 2c). Overall, we have a volume of investigation of 0.38 x 0.38 x 2 mm3, and can maintain nominal < 0.8 mm resolution inside 0.38 x 0.38 x 0.6 mm3.

Biosamples

Samples at realistic densities could be imaged without filtration or dilution. To study environmental bacteria on the order of 1 μm in their largest dimension, pure cultures were imaged in optimal conditions. Fig. 3 shows phase and intensity images of three test strains: (a) E. coli, (b) V. alginolyticus, and (c) B. subtilis. The phase images showed slightly more contrast and were more readily used for tracking. Although the individual bacteria were difficult to identify in still images, their motion was very clear in real time. B. subtilis spores (mean length, 1.1 ± 0.1 μm; width, 0.48 ± 0.04 μm) could be readily resolved in phase (Fig. 3c inset). (11)

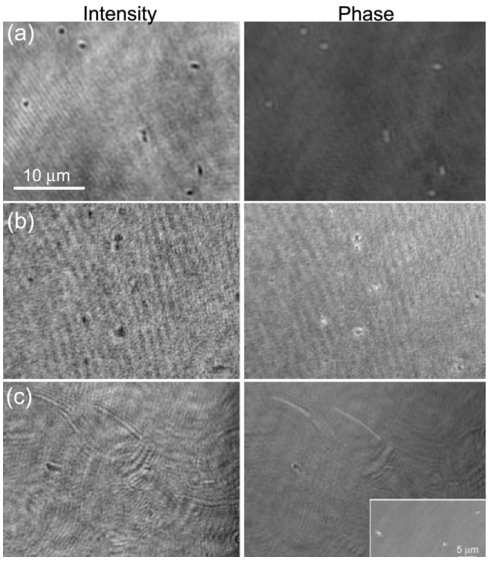

Figure 3. Images of bacteria amplitude (left) and phase (right). Cell densities represent approximate optical densities of 0.05 (organisms per pixel) for (A) E. coli, (B) V. alginolyticus, (C) B. subtilis vegetative cells and (inset) spores.

Bug Extraction

Blob Finding

For tracking, the software must be able to autonomously locate the organisms. While various programs were tested for this purpose, the algorithms employed by most programs are similar and can be done using Matlab. (10) Using the image processing tools, we averaged dynamic range over the whole stack for phase images. This enabled a constant mean value and removed image flicker over time. Then for each time-step, we increased contrast throughout, thresholded, and used background separation to locate individual bug cells as blobs. Using cell count, we recorded properties of each blob. This gave the dimensions and location shown in Fig. 4. All steps were repeated for the next time-step.

While the process worked very well for objects that were clearly distinct from the background, success rate with bugs was very low. For a sample bacterial image, false positives (non-bugs captured) was 86%, while false negatives (bugs not captured) was 69%, based on visual inspections. This led to our conclusion that improvement in contrast was necessary for better tracking results.

The results may differ slightly with volume, as each image generally contains traces of bugs along out-of-focus planes. In fact, bug accumulation over z causes further loss of contrast. To visualize bug accumulation in a region, overall bug paths can be generated for individual 2D stacks by integrating images over time and normalizing. By combining multiple 2D tracks and scaling the RGB values by depth, the 3D set can be used to generate tracks with colour-scaled depth as shown in Fig. 4 (available: msurj.mcgill.ca/Vol10_1.php).

Quantum Dots

Colloidal Quantum Dots (QDs) are semiconductor nanocrystals whose photoluminescence emission wavelength is proportional to the size of the crystal. (11) Their outer surfaces can be readily conjugated to organic molecules; they are therefore useful as biological labels. (12) Their use in DHMs is, however, not well studied and could suggest a new method for contrast improvement, leading to better tracking abilities.

To test the efficiency of QDs as holographic dyes, we grew multiple batches of E.coli together. While we grew one batch under normal conditions as a control, we conjugated another batch with QDs upon reaching half-log growth phase. We then imaged both sample sets and analyzed the images for discernible differences.

Since both samples were cultured from the same source and imaged at equal growth time at equal volume and concentration, they can be assumed to have an equal number of live E.coli. Any difference between the observed numbers of bacteria in Fig. 5 can then be associated with the inclusion of QDs.

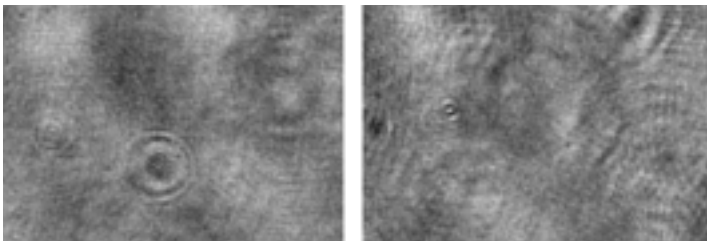

Figure 5. Amplitude reconstructions for E.coli sample without (left) and with (right) QD conjugation. Samples were imaged under similar conditions and can be assumed to have equal bug concentration. While individual bugs may be difficult to identify in the images, an overall increase in contrast and variance can be noticed.

To quantitatively measure the change in contrast, we defined contrast ratio as the difference between the maximum and minimum intensity of pixels within a given range. We normalized the dynamic range for all images between 0 and 255, and we analyzed a cross section along y (at fixed x) for contrast ratio. This let us plot contrast ratio (against x coordinate as location) for each set of image as shown in Fig. 6 (image available: msurj.mcgill.ca/Vol10_1.php).

By averaging the measurements over x and t, we calculated average contrast ratio to be 131 (±3) for the control sample and 143 (±5) for the QD sample, thus leading to a 9% increase in contrast ratio. Repeating the measurements with x and y interchanged yielded similar results: 128 for the control sample and 145 for the QD sample, resulting in a 13% increase. Therefore, it can be seen that there is a small but definite increase in contrast with the use of Quantum Dots.

Conclusion

The dual-beam, off-axis holographic microscopy can be used to image

bacteria in the micron range. The MZ interferometer instrument has a 380 x 380 x 600 (μm) three-dimensional field of view and can maintain nominal < 0.8 mm resolution within this volume. However, the contrast between bug and background is not optimal for tracking and leads to a false positive rate of around 86% currently.

Conjugation of the bugs with Quantum Dots increases the contrast ratio as defined by 11.26 (±2.06) %. While this change is not large, it does suggest that use of Quantum Dots can increase the contrast for Digital Holographic Microscopes. In further study, we hope to replace the bacteria with micron-size beads and image the samples with and without Quantum Dot conjugation. Unlike live bacteria, the beads will have a fixed concentration which can be found to a high precision, and can be used to quantify change in contrast with QD ratio.

In an additional venue towards improvement, the hardware team behind the microscope is attempting to reduce aberrations present in the current system to improve contrast, which should allow for better imaging and tracking results. A more compact system, named the Common Mode, is being designed. This system includes collimated optical paths instead of an MZ interferometer. Assuming that these changes improve imaging capabilities and allow for successful tracking, the microscope will be applicable in various fields and can be used remotely for studies of microbial organisms.

Acknowledgements

I would like to thank Dr. Jay Nadeau, who has constantly been helpful and supportive during this research. I would also like to thank the research team at the California Institute of Technology , who designed and created the MZ microscope. This work was supported by the Gordon and Betty Moore Foundation through grants to the California Institute of Technology and McGill University. The instrument was installed and tested for workability during the summer period. The post-processing of image stacks and the study for extraction and contrast were done in the fall semester.

References

1. Cuche E, Marquet P, Depeursinge C. Simultaneous amplitude-contrast and quantitative phase-contrast microscopy by numerical reconstruction of Fresnel off-axis holograms. Applied Optics. 1999;38(4):6994-7001.
2. Kim MK. Principles and techniques of digital holographic microscopy. SPIE Reviews. 2010;1.
3. Dubois F, Joannes L, Legros JC. Improved three-dimensional imaging with a digital holography microscope with a source of partial spatial coherence. Applied Optics. 1999;38(34):7085-7094.
4. Cuche E, Emery Y, Montfort F. Microscopy: one-shot analysis. Nature Photon. 2009;3:633-635.
5. Kreis TM. Frequency analysis of digital holography. Optical Engineering. 2002;41(4):771-778
6. Matsushima K, Schimmel H, Wyrowski F. Fast calculation method for optical diffraction on tilted planes by use of the angular spectrum of plane waves. Journal of the Optical Society of America A; Optics, Imagine Science, and Vision. 2003;20(9):1755-1762.
7. de Nicola S, Finizio A, Pierattini G, Ferraro P, Alfieri D. Angular spectrum method with correction of anamorphism for numerical reconstruction of digital holograms on tilted planes. Optics Express. 2005;13(24):9935-9940.
8. Mann C, Yu L, Lo CM, Kim M. High-resolution quantitative phase-contrast microscopy by digital holography. Optics Express. 2005;13(22):8693-8698.
9. Colomb T, Cuche E, Charrière F, Kühn J, Aspert N, Montfort F, Marquet P, Depeursinge C. Automatic procedure for aberration compensation in digital holographic microscopy and applications to specimen shape compensation. Applied Optics. 2006;45(5):851-863.
10. Oku H, Ogawa N, Ishikawa M, Hashimoto K. Two-dimensional tracking of a motile micro-organism allowing high-resolution observation with various imaging techniques. Review of Scientific Instruments. 2005;76(3): 034301.
11. Kloepfer J, Mielke R, Wong M, Nealson K, Stucky G, Nadeau JL. Quantum dots as strain- and metabolism-specific microbiological labels. Applied and Environmental Microbiology. 2003;69(7):4205-4213.
12. Bruchez M, Moronne M, Gin P, Weiss S, Alivisatos A. Semiconductor Nanocrystals as Fluorescent Biological Labels. Science. 1998;281(5385):2013-2016.